*Geotechnics for Catastrophic Flooding Events – Iai (Ed)*
*© 2015 Taylor & Francis Group, London, ISBN 978-1-138-02709-1*

# Damage to river levees by the 2011 Off the Pacific Coast Tohoku earthquake and prediction of liquefaction in levees

M. Okamura
*Ehime University, Matsuyama, Japan*

S. Hayashi
*Kobe Electric Railway Co. Ltd.,Kobe, Japan*

ABSTRACT: More than 2000 river levees were damaged by the 2011 Off the Pacific Coast of Tohoku Earthquake and liquefaction of soils in levees is considered to be the fundamental mechanism of about 80% of the damaged levees. Vulnerability assessment of existing levees and execution of remedial countermeasure for this newly realized mechanism will be the next challenge. In this study the validity of the liquefaction evaluation method used in the current practice was examined. It was revealed that the current method provides the factor of safety against liquefaction, $F_L$, for relatively thin saturated layers in levees excessively on the safe side. A possible reason for this is considered to be drainage of generated excess pore pressure during the earthquake shaking. An attempt was made to improve the liquefaction evaluation method by taking the drainage effects into account.

## 1 INTRODUCTION

In order to fight against riverine flooding that has continued to produce devastating consequences, in both life and economic losses, several tens of thousands of kilometers of river levees have been constructed over centuries since the Edo era in Japan. Even though the construction efforts have been continuously devoted, approximately 40% of levees in Japan does not have enough height and width. Raising and widening the levees still have a highest priority in the current engineering practice of river levee management.

On the other hand, although river levees have repeatedly been damaged by earthquakes, it was rarely the case that the damage to levees resulted in devastating consequences of flooding, and thus seismic effects on levees had not been considered in the engineering practice. In 1995, Hogoken-nambu earthquake caused severe damaged to the levees of the Yodo river and Osaka city, the second largest city of Japan, was in real danger of flooding. Thick loose alluvium sand deposits liquefied and the 5 m high levees subsided as much as 3 m. Since the dominant mechanism of the seismic damage to levees in past large earthquakes was believed to be the liquefaction of foundation soils, execution of liquefaction countermeasure for foundation soils of vulnerable levees has started after the Hyogoken-nambu earthquake.

Regarding the seismic damage, occurrence of crest settlement larger than half of the embankment height is not unusual when foundation soils liquefy (Matsuo, 1999). Levees resting on non-liquefiable soil, however, were considered to have rarely experienced severe damage. Recorded crest settlement due to the deformation of soft foundation clay was, at the largest, 15% of the levee height (River Front Center, 1999). In 1993, the Kushiro-oki earthquake hit the northern part of Japan and the Kushiro river levees were severely damaged. The incident attracted attention of engineers since damaged levees were underlain by a non-liquefiable peat deposit. It was presumed that the surface of the highly compressible and less permeable peat deposits below the levees had subsided in a concave shape, creating saturated zone in the levees, as shown in Figure 1 (Sasaki et al., 1995). More recently, more than 2000 river levees were damaged by the 2011 off the Pacific Coast of Tohoku Earthquake (River Bureau, Ministry of Land, Infrastructure and Transport, 2011) and a considerable number of levees failed in this mechanism. Assessment of vulnerable existing levees and execution of countermeasure for this newly realized mechanism will be a next challenge.

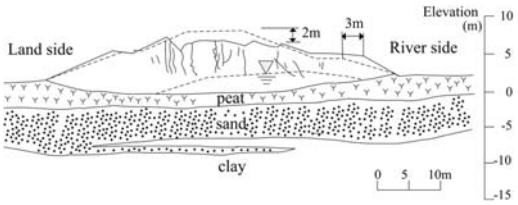


Figure 1. Damaged levee of the Kushiro river (Sasaki et al., 1995).

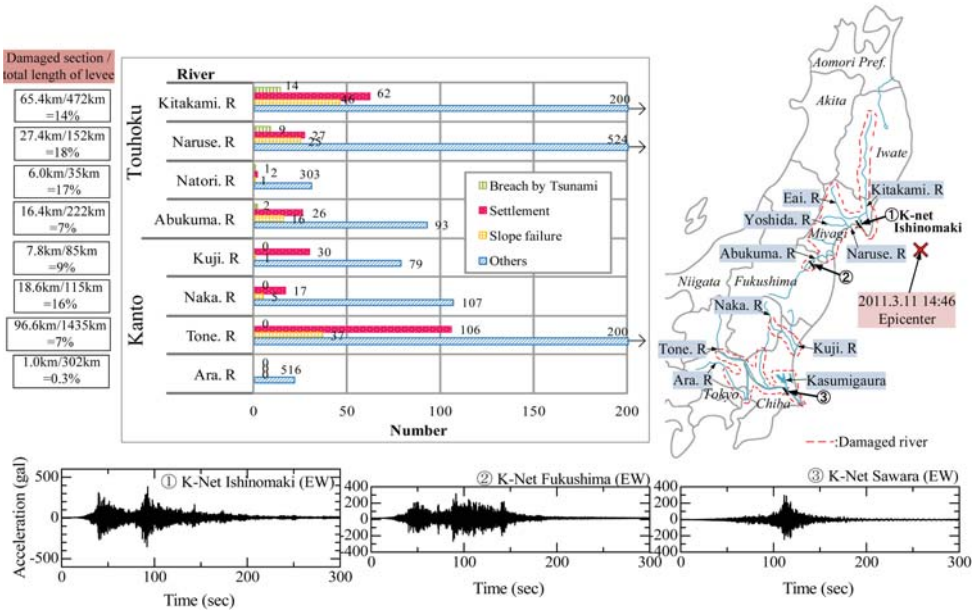


Figure 2. Locations and number of damaged levees caused by the 2011 Off the Pacific coast Tohoku Earthquake (after River Bureau of MLIT, 2011).

## 2 LIQUEFACTION IN LEVEES BY 2011 OFF THE PACIFIC COAST TOHOKU EARTHQUAKE

The Off the Pacific Coast Tohoku Earthquake of moment magnitude 9.0 occurred on March 11, 2011, with its hypocenter located at 130 km from the coast and a depth of 24 km. Figure 2 shows locations and the number of damaged levees as well as typical acceleration time histories observed with K-Net. Maximum accelerations of the main shock observed in coastal areas of soft soil profiles ranged from about 0.3 g to 0.6 g in the Tohoku district and from about 0.2 g to 0.4 g in the Kanto district. The main shock lasted more than 2 minutes, followed by a large number of aftershocks. 416 aftershocks of moment magnitude higher than 5.0 were recorded by the end of March 2011, in 20 days after the main shock. A total of some 2000 damaged river levees extended widely from northern part of Iwate Prefecture to Tokyo as indicated with the broken lines in the figure and a total length of damaged levee sections added up to 241 km. On heavily damaged levees which no longer had a function to resist high-water, such as levees with crest height lower than high-water level or those with significant cracks and deformation, detailed in-situ investigation was conducted including SPT, CPT, Swedish weight sounding, ground water level monitoring, sampling and laboratory tests and even direct observation by completely dissecting levees. It was confirmed that soil liquefaction was the dominant mechanism to cause the heavy damage. From a viewpoint of locations of liquefied soil layers, damaged levees are broadly classified into three types as illustrated in Figure 3. The first one is such that a liquefied soil layer existed in the levee on a thick clay deposit; the second one is such that the liquefied sand layer existed only in the foundation soil and the levee was consisted of non-liquefiable soil; and the third type is the combination of the first and the second. For type 1 levees, the surface of the compressible and less permeable clay deposit below the levee had subsided in a concave shape, creating a saturated zone in the leveeas shown in Figure 1. For such levees, expected deformation mechanisms is lateral spreading of levees with limited deformation of foundation soil. Figure 4 depicts the toe of such levee where the levee spread laterally on the surface of foundation soil towards hinterland side without any noticeable deformation detected on the ground surface outside the levee toe.

The number of levee failed in the first and third mechanisms was some 80% of the damaged levees. Liquefaction of soils in levees was certainly the dominant mechanism.

Figure 5 illustrates a cross section of such a damaged levee, the left bank levee of the Naruse river at 30.3 km from the mouth, which was originally approximately 9 m high and rested on a thick alluvium clay deposit (Tohoku Regional Development Bureau, MLIT, 2011). The water table in the levee observed 7 weeks after the earthquake with excavated boreholes was more than 2 m above the foundation clay layer (Ac1), indicating that the lower part of the levee (Bs) was saturated. The soils of the levee (Bs) was mostly silty sands with the SPT N-values lower than 5. The levee spread laterally on the rice pad which remained

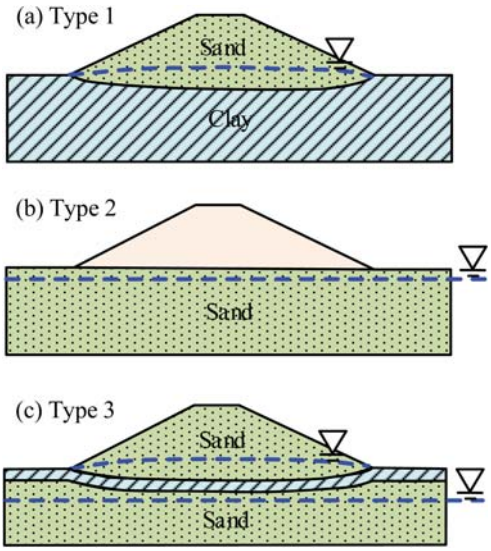


Figure 3. Three types of levee and foundation soil classified based on location of liquefied soil layers (TRDB, 2011).

Figure 4. Naruse River, R12.0k (River division, NILM). The levee spread laterally on the surface of foundation soil toward hinterland side. There was not any detected deformation outside the levee toe.

intact and many cracks and fissures appeared on the slope were partly filled with boiled sand. All these facts suggest that the levee liquefied. It is interesting to note that neighboring undamaged levees and their foundation soil conditions were quite similar to those of the damaged levees in all aspects with an exceptionof the water table in the levee being slightly lower (Tohoku Regional Development Bureau, MLIT, 2011). The loose saturated soil layer at the base of the levee with a thickness of about 2 m in the damaged section liquefied and caused serious damage to the levee, and the undamaged levees had the saturated soil with a smaller thickness which presumably did not liquefy. This alludes effects of drainage of pore water from saturated soil layers on occurrence of liquefaction and severity of damage.

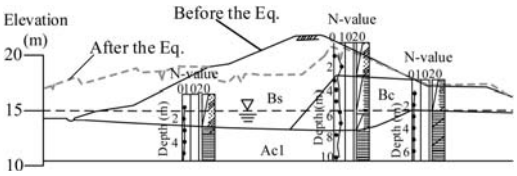


Figure 5. Damaged levee of the Naruse river (TRDB, Ministry of Land, Infrastructure and Transport, 2011.

## 3 LIQUEFACTION ASSESSMENT OF DAMAGED AND UNDAMAGED LEVEES

In order to assess vulnerability to liquefaction of levees, the validity of the evaluation method of in-situ liquefaction susceptibility is important. In this chapter, the liquefaction evaluation method used in the current practice is examined.

The author picked out 18 severely damaged levees where liquefaction of soils inside the levees are considered as a main cause of damage (the first type in Figure 3). Another 12 undamaged levees in the neighborhood of those damaged levees were also selected and their properties are summarized in Table 1. Figure 6 depicts variation in crest settlement and soil profile in the longitudinal direction of a typical section containing damaged and undamaged levees. Subsided and cracked significantly in the section between 30.9 k and 31.6 k, the levee in the section between 30.6 k and 30.9 k practically suffered from no damage despite conditions were similar in all aspects including levee height, foundation clay thickness, SPT-N values and soil type with an exception of the thickness of saturated zone in the levees. The saturated levee soil had evidently larger thickness in the heavily damaged section than the slightly damaged and non-damaged section.

The safety factors against liquefaction, $F_L$ ($=R_L/L$), of all the 30 levees were calculated with the method of the Japan Road Association (JRA, 2012). SPT-N values and fines content obtained at the sites after the earthquake were used to estimate the liquefaction resistance of the soils, $R_L$. These levees have been built up and extended over decades without following modern standards and construction technique, the levee soils were generally loose. The normalized SPT-N values, $N_1$ ($=(170N/(70+\sigma'_v))^{0.5}$), of the saturated soil layers were in a range between 0 and 10, as indicated in Figure 7. Distribution of $N_1$ values of damaged and undamaged levees are quite similar to each other and $N_a$ values, the normalized $N$ value with the effects of fines content taken into account, are also the case.

Cyclic stress ratio developed at the sites, $L$, were estimated from following equation,

$$L = c_w \frac{a_{\max}}{g} \frac{\sigma_v}{\sigma_v'} r_d \qquad (1)$$

where $\sigma_v$ and $\sigma'_v$ denote the total and effective vertical overburden stress calculated simply using overlying soil thickness, respectively, and $a_{\max}$ is the maximum ground acceleration. Because of the large moment

Table 1. Summary of damaged and undamaged levees used for validation of $F_L$ methods.

| No. | River | Location* | Levee height m | Crest settlement m | Thickness of saturated layer m | $D_{10}$ mm | Permeability k (Hazen) m/s | $N$ | $N_1$ | $N_a$ | FC % | Estimated max acc. gal |
|---|---|---|---|---|---|---|---|---|---|---|---|---|
| (a) Damaged levee | | | | | | | | | | | | |
| 1 | Abukuma | R22.5k + 70 (H) | 5.8 | 2.2 | 2.2 | 0.0090 | $1.1 \times 10^{-4}$ | 3 | 4 | 6.5 | 29 | 341 |
| 2 | | L28.8 + 85k (H) | 4.6 | 0.2 | 2.3 | 0.0020 | $3.0 \times 10^{-6}$ | 2 | 3 | 3.3 | 15 | 341 |
| 3 | | R31.0k + 50 (H) | 5.7 | 2.0 | 2.4 | 0.0100 | $1.3 \times 10^{-4}$ | 3 | 4 | 8.2 | 39 | 341 |
| 4 | | R32.9k + 70 (H) | 6.6 | 1.1 | 2.5 | 0.0130 | $2.3 \times 10^{-4}$ | 3 | 4 | 6.4 | 32 | 341 |
| 5 | Naruse | L11.5k (H) | 5.6 | 2.4 | 1.7 | 0.1020 | $1.4 \times 10^{-2}$ | 3 | 6 | 11.2 | 31 | 657 |
| 6 | | R12.0k (C) | 5.4 | 0.9 | 3.8 | 0.0070 | $6.5 \times 10^{-5}$ | 1 | 1 | 4 | 48 | 657 |
| 7 | | R12.0k (H) | 5.4 | 0.9 | 3.3 | 0.0070 | $6.5 \times 10^{-5}$ | 3 | 4 | 7.7 | 40 | 657 |
| 8 | | R12.0k (R) | 5.4 | 0.9 | 2.6 | 0.0070 | $6.5 \times 10^{-5}$ | 2 | 3 | 4.1 | 20 | 657 |
| 9 | | L29.1k (R) | 6.2 | 2.6 | 0.9 | 0.0100 | $1.3 \times 10^{-4}$ | 3 | 6 | 7.5 | 21 | 568 |
| 10 | | L30.3k (H) | 7.5 | 5.5 | 2.9 | 0.0015 | $3.0 \times 10^{-6}$ | 2 | 4 | 14.3 | 75 | 568 |
| 11 | Yoshida | L14.8k (C) | 7.8 | 1.5 | 2.8 | 0.0100 | $1.3 \times 10^{-4}$ | 6 | 5 | 7.9 | 31 | 657 |
| 12 | | L14.8k (R) | 7.8 | 1.5 | 1.2 | 0.0100 | $1.3 \times 10$v-4 | 3 | 4 | 8.9 | 47 | 657 |
| 13 | Eai | R14.15k (C) | 4.1 | 1.5 | 3.0 | 0.0015 | $3.0 \times 10^{-6}$ | 1 | 1 | 4.6 | 56 | 463 |
| 14 | | R14.35k (C) | 4.3 | 1.3 | 1.7 | 0.0020 | $5.3 \times 10^{-6}$ | 0 | 0 | 2.5 | 55 | 463 |
| 15 | | L14.4k (C) | 3.0 | 1.4 | 1.1 | 0.0045 | $2.7 \times 10^{-5}$ | 1 | 1 | 3.2 | 36 | 463 |
| 16 | | L14.61k (C) | 4.0 | 1.2 | 3.6 | 0.0050 | $3.3 \times 10^{-5}$ | 1 | 1 | 3.9 | 45 | 463 |
| 17 | | L27.7k (C) | 3.4 | 2.5 | 2.2 | 0.0150 | $3.0 \times 10^{-4}$ | 3 | 4 | 2.4 | 0 | 326 |
| 18 | Shin eai | R2.8k + 40 (C) | 6.7 | 1.4 | 1.9 | 0.0020 | $5.3 \times 10$-6 | 4 | 4 | 11.7 | 64 | 568 |
| (b) Undamaged levee | | | | | | | | | | | | |
| 1 | Abukuma | L29.123k (C) | 4.6 | 0 | 0.6 | 0.0130 | $2.3 \times 10^{-4}$ | 10 | 10 | 13.7 | 26 | 341 |
| 2 | | L28.75k (C) | 4.6 | 0 | 1.2 | 0.0130 | $2.3 \times 10^{-4}$ | 12 | 11 | 15 | 29 | 341 |
| 3 | Naruse | L11.7k (H) | 5.6 | 0 | 0.4 | 0.0100 | $1.3 \times 10^{-4}$ | 4 | 6 | 11 | 37 | 341 |
| 4 | | R11.9k (C) | 5.4 | 0 | 2.9 | 0.0100 | $1.3 \times 10^{-4}$ | 4 | 6 | 11.2 | 37 | 657 |
| 5 | | R29.0k (R) | 6.8 | 0 | 0.5 | 0.0020 | $3.0 \times 10^{-5}$ | 3 | 5 | 19 | 81 | 657 |
| 6 | | L30.7k (H) | 7.0 | 0 | 0.5 | 0.0020 | $5.3 \times 10^{-6}$ | 2 | 3 | 12 | 75 | 568 |
| 7 | Yoshida | L14.9k (C) | 7.8 | 0 | 1.8 | 0.0100 | $1.3 \times 10^{-4}$ | 2 | 2 | 5.1 | 47 | 568 |
| 8 | | L15.3k (H) | 8.4 | 0 | 1.7 | 0.0060 | $4.8 \times 10^{-5}$ | 2 | 3 | 12 | 75 | 657 |
| 9 | Eai | L14.7k (H) | 4.0 | 0 | 0.5 | 0.102 | $1.4 \times 10^{-2}$ | 3 | 4 | 4.2 | 15 | 463 |
| 10 | | R26.69k (C) | 3.8 | 0 | 0.6 | 0.010 | $1.3 \times 10^{-4}$ | 3 | 3 | 10.8 | 65 | 326 |
| 11 | | L27.9k (H) | 3.4 | 0 | 0.6 | 0.008 | $8.5 \times 10^{-5}$ | 8 | 10 | 14 | 29 | 326 |
| 12 | Kitakami | L5.2k + 2 (C) | 4.7 | 0 | 2.2 | 0.052 | $3.6 \times 10^{-3}$ | 6 | 6 | 6.3 | 11 | 398 |

Location* C: crest, H: hinterland side slope R: riverside slope

magnitude and the large number of significant acceleration cycles contained in the main shock of the earthquake, the correction factor $C_w$ was assumed to be unity for the first approximation (Tokimatsu and Yoshimi, 1983; Idriss & Boulanger, 2006). The stress reduction factor $r_d$ was also assumed to be unity since the elevation of the soil layer to be assessed was similar to that of level ground surface.

Maximum ground accelerations at each levee were invoked based on those estimated by the National Institute for Land and Infrastructure Management (EDPD, 2012). EDPV has analyzed acceleration data recorded at strong motion seismograph observatories of K-NET, Kik-NET (National Research Institute for Earth Science and Disaster Prevention) as well as MLIT, and provided the interpolated maximum ground accelerations at a small interval. The factor of safety against liquefaction, $F_L$, is indicated in Figure 8. Being lower than unity for both damaged and undamaged levees, the factors of safety are not a good index to distinguish damaged levees from non-damaged levees.

It is of interest to note that the factors $F_L$ lower than unity are inevitable for cases of such a sever event with peak accelerations higher than 300 gals, those 12 levees survived without any noticeable damage. A possible explanation to the fact may be that the soils in the saturated zones of those levees did not liquefy probably because generated excess pore pressures dissipated swiftly during earthquake owing to shorter drainage distances and higher permeability of soils. Okamura & Tamamura (2010) and Okamura et al. (2012)conducted a series of dynamic centrifuge tests on embankments with thin saturated liquefiable zones at the base, with the thickness ranging between 0.8m and 1.2m and with the different drainage boundary conditions. They demonstrated that crest settlement of the embankment due to the shaking increased with an increase in the thickness of the saturated zone, with

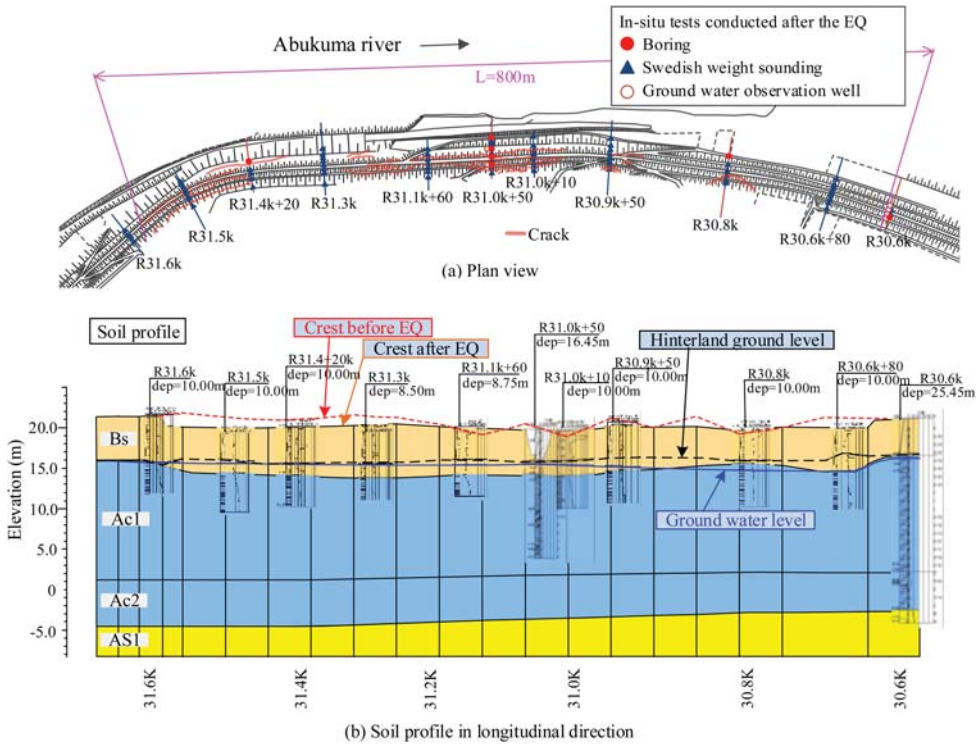


Figure 6. Variations of ground water level and soil profile in longitudinal direction of damaged levee.

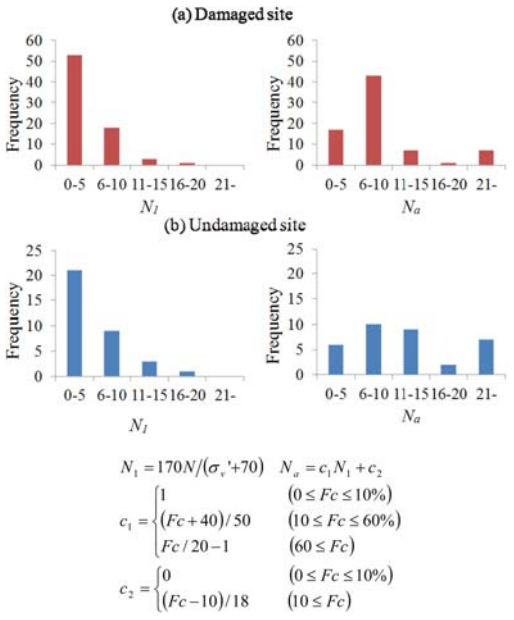


Figure 7. Frequency distribution of $N_1$ and $N_a$ values.

the settlement being larger for the zone with undrained boundaries. In the following sections, in order to verily the hypothesis that undamaged levees were survived due largely to the drainage effects, the drainage effects on the liquefaction potential of thin sand layers is studied in the following sections.

## 4 CENTRIFUGE TEST

In this section, a series of centrifuge tests performed in this study is described which aimed to investigate how the drainage during shaking affects pore pressure responses and accelerations needed to liquefy relatively thin sand layers.

### 4.1 *Model preparation and test condition*

Two types of models shown in Figure 9 were tested in a centrifuge at 25 g. The model 1 consisted of a 1m deep uniform sand deposit with the ground water table coincided to the ground surface, while the model 2 was the uniform sand deposit with the same density as model 1 and with the thickness two times larger than that of model 1. The ground water table was at 1m deep from the ground surface.

The soil used to build the models was Toyoura sand of which index physical properties are $\rho s = 2.64$, $e_{max} = 0.973$ and $e_{min} = 0.609$. Dry Toyoura sand was rained through air to a relative density of 45% or 70% in a rigid container with internal dimensions of 420 mm in width and 120 mm in length. During the sample preparation, accelerometers and pore pressure cells were installed at the locations indicated in the

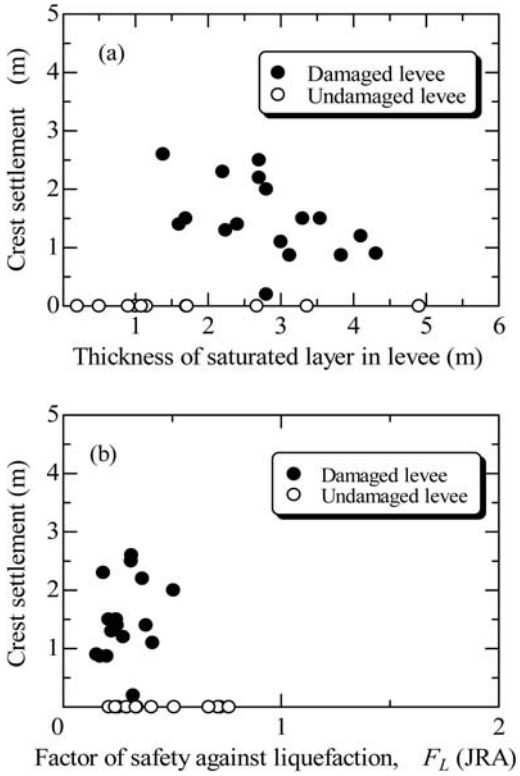


Figure 8. Variations in factor of safety assessed with JRA method and thickness of saturated layer in levees.

figure. For model 2, 5 mm thick sponges were glued on the side walls to allow the upper unsaturated sand layer to displace horizontally during shaking.

The models were fully saturated with water or viscous fluid in a vacuum chamber at a vacuum pressure of −95 kPa with the aid of $CO_2$ replacement technique to a degree of saturation higher than 99.5%, which was measured with the method developed by Okamura & Kitayama (2008) and Okamura & Inoue (2010). The viscous fluid was a mixture of water and hydroxypropyl methylcellulose (Type 65SH-50), termed Metolose by the Shin-etsu Chemical Company. In this study viscosity of Metolose solution was varied from 5cSt to 1000cSt by changing the concentration of the solution. The consequence of using the pore fluid with a viscosity $\nu$ times higher than that of water in the centrifuge tests at 25 g to model the liquefaction of the water-saturated prototype soil in the field is that the actual prototype permeability being simulated was $k_{\text{prototype}} = k_{\text{model}}/\nu$*25 (Tan & Scott, 1985). The coefficients of permeability of Toyoura sand $k_{\text{model}}$ are $2.5 \times 10^{-4}$ m/s at $Dr = 45\%$ and $1.8 \times 10^{-4}$ m/s at $Dr = 70\%$.

The model was set on the geotechnical centrifuge at Ehime University and the centrifugal acceleration was gradually increased to 25 g. For model 2, the pore fluid was drained through a stand pipe until the ground

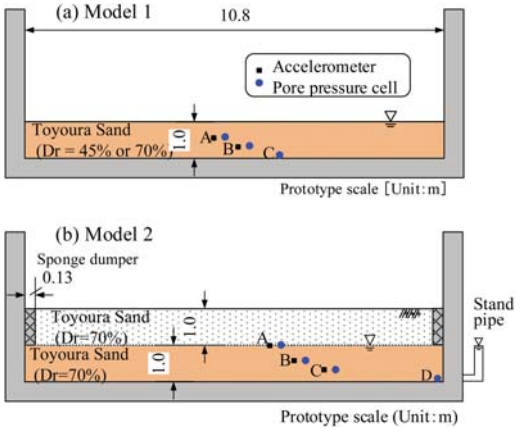


Figure 9. Centrifuge model configurations.

water table stabilized at the proper height. Horizontal base shaking was imparted to the models with a mechanical shaker, with the basic shape of acceleration time histories shown in Figure 12. The shaking intensity was varied by changing the rotation rate of a cam shaft in the shaker. The predominant frequencies of input motions were, for instance, 0.64 Hz for $a_{\max} = 0.8\,\text{m/s}^2$ and 1.0 Hz for $a_{\max} = 1.7\,\text{m/s}^2$. Test conditions are summarized in Table 2.

### 4.2 *Result and discussion*

Figure 10 shows typical time histories of acceleration and excess pore pressure responses during shaking observed in tests of model 1 with $Dr = 70\%$. The excess pore pressures depend apparently on the permeability, $k_{\text{prototype}}$; the model with $k_{\text{prototype}} = 6.4 \times 10^{-5}$ m/s liquefied in a few cycles of shaking with an acceleration amplitude 140 gal, while the model with the higher permeability $k_{\text{prototype}} = 5.0 \times 10^{-4}$ m/s needed a higher acceleration of 205 gal to liquefy. This clearly suggest that permeability of the soil and thus drainage has significant effects of liquefaction behavior of the soil layers. The maximum acceleration amplitudes of the input motions until the soil liquefied are plotted against the prototype permeability for all tests of models 1 and 2 in Figure 11. For cases of model 1, the acceleration amplitudes seems to be constant for $k_{\text{prototype}}$ lower than $10^{-5}$ m/s and increases with increasing $k_{\text{prototype}}$ for the higher permeability, with the acceleration amplitude being higher for higher relative density.

It should be mentioned in Figure 10 that the more permeable sand layer needed the higher acceleration to liquefy and the liquefaction lasted shorter duration. The excess pore pressure of the model with $k_{\text{prototype}} = 5.0 \times 10^{-4}$ m/s started to decrease about 5 seconds after the sand liquefied even though the shaking continued, while for the model with $k_{\text{prototype}} = 6.4 \times 10^{-5}$ m/s the liquefaction lasted more than 15 seconds. Liquefied soil is capable of continuously developing large cyclic shear strains even under

Table 2. Centrifuge test conditions represented in prototype scale.

| Model | *Dr* % | Viscosity of pore fluid, $\nu$ cSt | $k_{\text{prototype}}$ m/s | Input acc. amplitude, $a_{\max}$ gal | Frequency Hz | Number of cycles to liquefy |
|---|---|---|---|---|---|---|
| Model 1 | 45 | 1 | $6.3 \times 10^{-3}$ | 255 | 1.2 | 3 |
| | | 5 | $1.3 \times 10^{-3}$ | 169 | 1.0 | 2 |
| | | 10 | $6.3 \times 10^{-4}$ | 152 | 1.0 | 3 |
| | | 24 | $2.6 \times 10^{-4}$ | 112 | 0.84 | 2 |
| | | 120 | $5.2 \times 10^{-5}$ | 104 | 0.74 | 4 |
| | | 120 | $5.2 \times 10^{-5}$ | 73 | 0.64 | 7 |
| | | 500 | $1.3 \times 10^{-5}$ | 81 | 0.68 | 7 |
| | | 1000 | $6.3 \times 10^{-6}$ | 82 | 0.64 | 8 |
| | 70 | 9 | $5.0 \times 10^{-4}$ | 205 | 1.1 | 3 |
| | | 18 | $2.5 \times 10^{-4}$ | 198 | 1.1 | 5 |
| | | 27.5 | $1.6 \times 10^{-4}$ | 198 | 1.1 | 11 |
| | | 50 | $9.0 \times 10^{-5}$ | 190 | 1.0 | 5 |
| | | 70 | $6.4 \times 10^{-5}$ | 140 | 0.92 | 4 |
| | | 220 | $2.0 \times 10^{-5}$ | 104 | 0.72 | 15 |
| | | 1000 | $4.5 \times 10^{-6}$ | 105 | 0.72 | 2 |
| Model 2 | 70 | 9 | $5.0 \times 10^{-4}$ | 455 | 2.0 | 2 |
| | | 29 | $1.6 \times 10^{-4}$ | 324 | 1.2 | 3 |

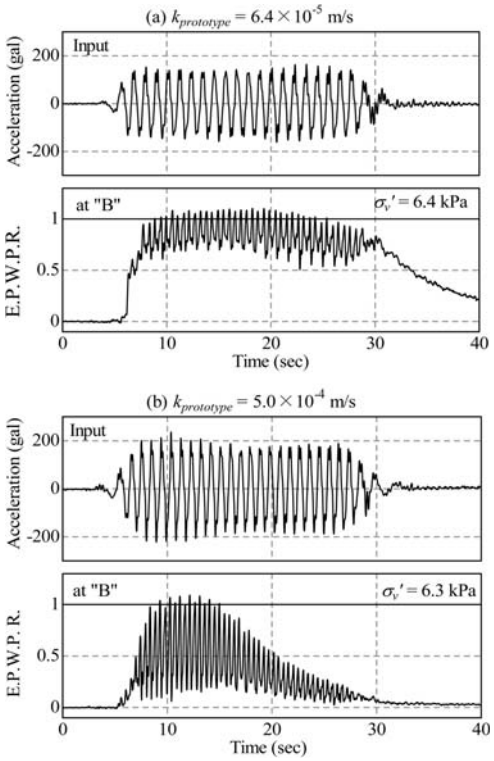


Figure 10. Typical acceleration and excess pore pressure time histories of Model 1 ($Dr = 70\%$).

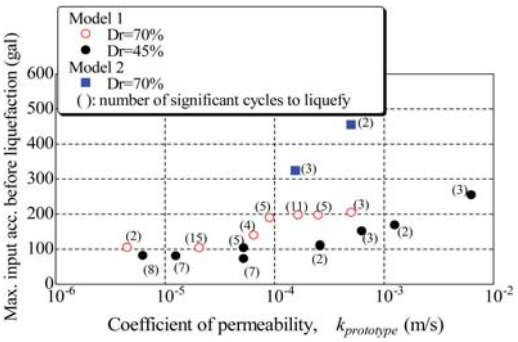


Figure 11. Variation in input acceleration to liquefy the sand layer with coefficient of permeability.

small accelerations. Okamura et al. (2001) has suggested that weak vibration or aftershocks acting on the already liquefied and continuously liquefied soil may contribute significantly to the continued deformation accumulation. For the cases of an earthquake with a long duration such as that shown in Figure 2, the permeability of sand must be a dominant factor on both the occurrence of liquefaction and the accumulated deformation.

The accelerations for model 2, in which liquefiable sand layers were overlain by unsaturated layers, are higher than those for model 1 as shown in Figure 11. Existence of the overlying unsaturated soil layer which decreased the cyclic stress ratio is responsible for this. Factors of safety against liquefaction $F_L$ for each tests were estimated as follows. Because of the different number of cycles to liquefy in each test as indicated in Figure 11, cyclic stress ratios corresponding to the number of cycles were employed as liquefaction resistance $R_L$,

$$R_L = CSR_{(N)} \frac{1 + 2K_0}{3} \tag{2}$$

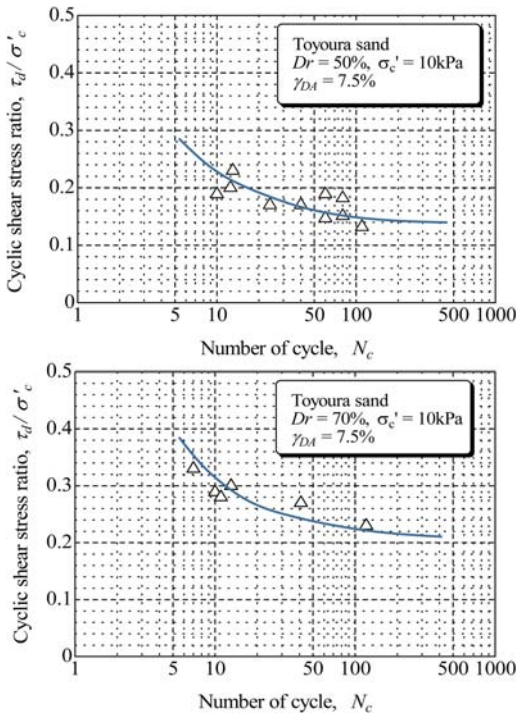


Figure 12. Liquefaction strengths obtained from torsional cyclic shear tests at low confining stress (Tanaka et al., 2009).

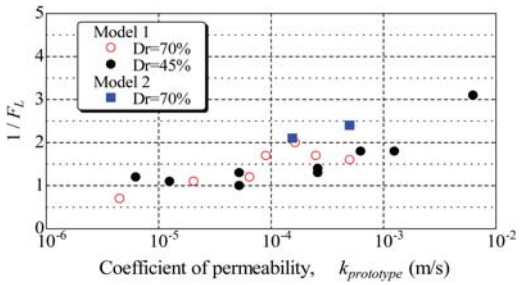


Figure 13. Variation in $1/F_L$ with permeability of sand.

where $CSR_{(N)}$ and $K_0$ denote the cyclic stress ratio at number of cycles N and the coefficient of earth pressure at rest (=0.5), respectively. Undrained cyclic torsional shear test results on Toyoura sand indicated in Figure 12 (Tanaka et al., 2009) were used for this purpose, of which test conditions were similar to those of the centrifuge including the initial effective confining pressure (10 kPa) and relative densities (50% and 70%). Maximum accelerations $a_{\max}$ used to estimate the cyclic stress ratio were the maximum input acceleration before the soils liquefied. The test results were approximated with liner relationships between cyclic stress ratio and number of cycles in log-log space (Liu et al., 2001) and indicated in the figure. The inverse of the factor of safety, $1/F_L$,is shown in Figure 13. $1/F_L$ is approximately unity in the range of $k_{\text{prototype}}$ lower than $10^{-5}$ m/s and increases with increasing $k_{\text{prototype}}$ regardless of the relative densities and the overburden pressure.

In model 2, the liquefied sand layers were overlain by unsaturated sand layers with a lower permeability, drainage at the surface of the liquefied layers might be impeded. It is well documented in the literature that overlying impermeable soil layers imposed the undrained condition to underlying soil layers (e.g. Kokusho & Kojima, 2002). In Figure 13, however, there are no distinct differences in $F_L$ value between model 1 and 2. In a saturated sand layer with overburden pressure, the hydraulic gradient will be significantly high at the surface of the layer, which might accelerate drainage at shallower depth. In fact, the excess pore pressure ratios at shallower location (labeled "A" in Figure 9(b)) of model 2 tend to be lower than locations B and C at the beginning of shaking, which was unlike model 1. The drainage boundary condition at the surface of liquefied soil layer of model 2 had little effects on drainage during the shaking.

## 5 VOLUMETRIC STRAIN DUE TO DRAINAGE

It is common practice to assume the undrained condition to access a potential for liquefaction, however, the centrifuge test results described above indicates that the undrained condition does not hold true depending on permeability. An apparent liquefaction resistance increased with increasing permeability and thus with amount of drained water from the layer during shaking. An increase in the apparent liquefaction resistance have also been observed in studies related to the membrane penetration and imperfect saturation of specimen (e.g. Chaney, 1978; Tokimatsu,1990; Yoshimi et al., 1988).

It is well recognized that unsaturated soils exhibit higher liquefaction resistance than fully saturated soils. The underlying mechanisms that enhance liquefaction resistances of the unsaturated sand is such that air in a partially saturated sand mass plays a role of absorbing generated excess pore pressures by reducing its volume (Okamura and Soga, 2006; Kazama et al., 2006; Unno et al., 2008).Okamura & Soga (2006) derived influential factors of the liquefaction resistance of a partially saturated sand from theoretical consideration and examined effects of the factors through a series of triaxial tests on a clean sand. They assumed that air in the soil contracted according to excess pore pressure and defined the potential volumetric strain, $\varepsilon_v^*$, as,

$$\varepsilon_v^* = \frac{\sigma_c'}{p_0 + \sigma_c'}\left(1 - S_r\right)\frac{e}{1+e} \tag{3}$$

where $S_r$ is degree of saturation, $\sigma_c'$ is initial effective confining pressure and $p_0$ is initial pore pressure (in absolute pressure). The potential volumetricstrain is a volumetric strain that will be attained when the excess pore pressure reaches its maximum value, the initial

effective stress. They found the unique relationship between liquefaction resistance ratios, *LRR*, that is the ratio of cyclic shear stress ratio for a sand to that of fully a saturated sand, and the potential volumetric strain as shown in Figure 14. They approximatedthe relation with the following equation.

$$LRR = \log\left(6500\,\varepsilon_v^{*} + 10\right) \tag{4}$$

Since the drainage during shaking and reducing pore volume of unsaturated soils, both result in the contraction in soil volume,may have similar effects on liquefaction resistance, an attempt is made in this study to estimate the amount of water expelled from the saturated sand layers during shaking and resulting volumetric strains. Being a direct and promising method, measurement of surface settlement in a good accuracy was difficult especially for the thin sand layers in the centrifuge. Amount of water to be drained during a time duration $t_d$ from a sand layer with a thickness $H$ with an impermeable boundary at the base is estimated as follows.

$$V_d = k \cdot i \cdot t_d \tag{5}$$

When the excess pore water pressure ratio of the sand layer reaches unity, hydraulic gradient attains its maximum value as,

$$i_{max} = \sigma_v'/\gamma_w \qquad H \tag{6}$$

The volumetric strain due to the drainage can be expressed as,

$$\varepsilon_{v\,\max} = \frac{k\sigma_v'}{\gamma_w H^2} t_d \tag{7}$$

where $\sigma_v'$ and $\gamma_w$ denotes the effective overburden pressure and the unit weight of water, respectively. In this calculation, $t_d$ is assumed as the time duration from the beginning of the significant acceleration cycle till the sand liquefied. Corresponding excess pore pressure ratios during the time duration were approximately from 30% and 100%.

The factors $1/F_L$ of the centrifuge models are plotted against the volumetric strain in Figure 15 together with *LRR*, the empirical relationship obtained from the cyclic triaxial tests on unsaturated sands. The centrifuge test results from different models at the different relative densities lay almost on a unique curve. Although the factors $1/F_L$ or the apparent liquefaction resistance begin to increase at lower volumetric strain than *LRR*, both $1/F_L$ and *LRR* increase in a quite similar tends. This strongly suggests that the drainage during shaking and the compression of air in soils, both allow volumetric contraction of soils, have similar effects on the liquefaction resistance. Possible causes for the difference between $1/F_L$ and *LRR* may be time duration $t_d$ and permeability coefficient em ployed in the calculation of volumetric strain.

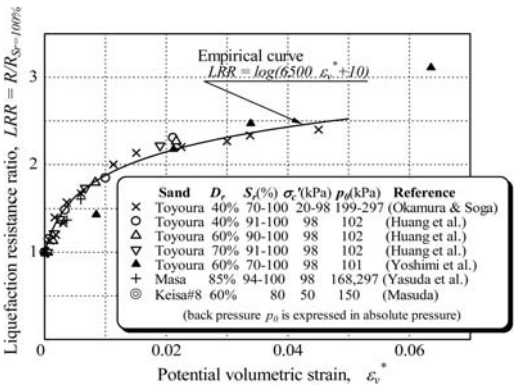


Figure 14. Relationship between hypothetical volumetric strain and liquefaction resistance of partially saturated sand (after Okamura & Soga, 2006).

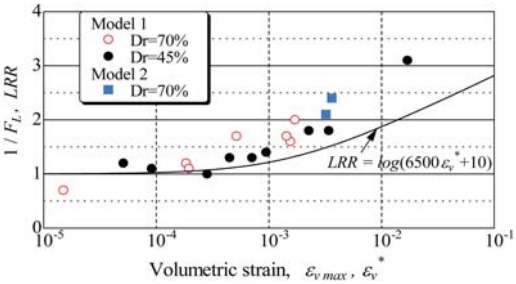


Figure 15. Relationship between rates of increase in apparent liquefaction resistance and volumetric strain due to drainage.

It should be mentioned here that there is a distinct difference in the flow of pore water depending on depth. The drainage effect arises as the result of upward flow of pore water towards the drainage boundary. A soil at the bottom of liquefied layer dissipates generated excess pore pressures by expelling the amount of water which is equivalent to the volume of contraction of soil skeleton, while for a soil at shallower depth amount of outflow water to dissipate excess pore pressure is amount of inflow water from underlying soil in addition to that equivalent to contraction of soil skeleton. For a uniform sand layer the amount of outflow water increases with decreasing the depth, while the flow rate is restricted by the permeability of soil. The resulting consequence is that liquefaction condition begins at the surface and propagates downward as observed in many 1g and centrifuge tests on saturated uniform sand deposits without overburden pressure (e.g. Dobry, 1995). Heterogeneous excess pore pressure ratio will be the typical case for thick deposits and excess pore pressures ratio distributes more or less uniformly in such thin sand layers as models tested in this study.

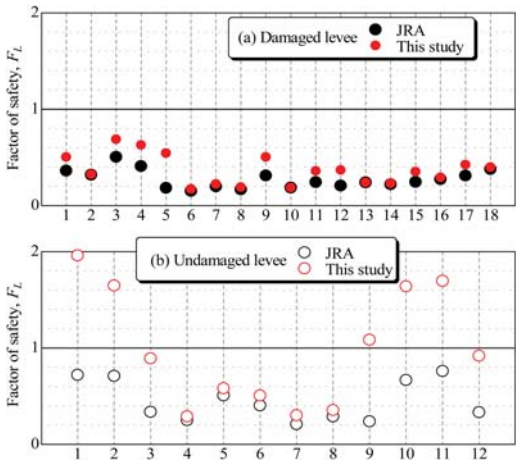


Figure 16. Factor of safety against liquefaction with and without taking drainage effect into account.

## 6 QUEFACTION ASSESSMENT CONSIDERING DRAINAGE EFFECT AND ITS VILIFICATION

Factor of safety $F_L$ of all the damaged and undamaged levees are evaluated again with taking the effect of drainage into account. Volumetric strain of liquefiable soils in each levees are calculated with equation (5) and the liquefaction resistance ratio, *LRR* derived from equation (4), was multiplied to $F_L$ value from JRA method already derived in the chapter 3. Coefficient of permeability was determined from grain-size data with the Hazen formula as,

$$k\,(\mathrm{m/s}) = 1.3D_{10}{}^{2} \qquad (9)$$

where $D_{10}$ is diameter of grains in the 10th percentile expressed in millimeters. The obtained factors of safety for all the 30 levees are shown in Figure 16.$F_L$ for undamaged levees significantly increased by taking the drainage effect into account; $F_L$ of seven levees out of 12 undamaged levees became higher than or almost equals to unity. While for the damaged levees, $F_L$ of all the levees stays below unity. The results of liquefaction susceptibility assessment was improved considerably by taking the damage effect into account especially for levees with relatively thin saturated layers.

## 7 CONCLUDING REMARKS

More than 2000 river levees were damaged by the 2011 Off the Pacific Coast of Tohoku Earthquake and liquefaction of soils in levees is considered to be the fundamental mechanism of about 80% of the damaged levees. Vulnerability assessment of existing levees and execution of remedial countermeasure for this newly realized mechanism will be the next challenge.

In assessing susceptibility to liquefaction of levees, the validity of the evaluation method of in-situ liquefaction susceptibility is important. In this study the validity of the liquefaction evaluation method used in the current practice was examined. Liquefaction assessment on eighteen damaged and twelve undamaged levees conducted in this study revealed that the current method provides the factor of safety against liquefaction, $F_L$, for relatively thin saturated layers in levees excessively on the safe side. Estimated factors $F_L$ for not only the damaged levees but also all the undamaged levees were lower than unity. A possible reason for this was considered to be drainage of generated excess pore pressure during the earthquake shaking. An attempt was made to improve the liquefaction evaluation method by taking the drainage effects into account.

A series of centrifuge tests was conducted on thin sand layers to investigate effects on shaking acceleration necessary to liquefy the layers of factors including relative density and permeability of sand and overburden pressures. The input acceleration necessary to cause liquefaction and thus an apparent liquefaction resistance increased with increasing permeability of the sand. Since the drainage of pore fluid is suggested to be responsible for the increase in the apparent liquefaction resistance, volume of drained fluid and the resultant volumetric strain before the sand liquefied was estimated. It was found that the apparent liquefaction resistance ratio increased uniquely with the volumetric strain due to the drainage.

It has been known that the liquefaction resistance of sands increases with degreasing degree of saturation. Existence of air allows nearly saturated sand to contract even in the undrained condition and this volumetric strain is believed to enhance the liquefaction resistance. It was found that the relationship between the apparent liquefaction resistance ratio and volumetric strain obtained from the centrifuge tests was in close similarity with that from undrained cyclic triaxial tests on unsaturated sands.

Liquefaction assessment with the effects of drainage taken into account was conducted for the damaged and undamaged levees by the 2011 earthquake. Results of assessment was much improved by considering the drainage effect. Factors of safety stayed lower than unity for all the damaged levees while factors were higher than unity for more than half of the undamaged levees.

## REFERENCES

Chaney, R.C. 1978. Saturation effects on the cyclic strength of sands, *Earthquake engineering and oil dynamics, GED, ASCE* 1: 342–358.

Dobry, R., Taboada, V. & Liu, L. 1995. Centrifuge modeling of liquefaction effects during earthquakes, *Proc. 1st Int. Conf. on Earthquake Geotechnical Engineering* 3: 1291–1324.

Ishihara, K., Iwamoto, S., Yasuda, S.& Takatsu, H. 1977. Liquefaction of anisotropically consolidated sand. *Proc. the*

*Ninth International Conference on Soil Mechanics and Foundation Engineering, Tokyo* 2: 261–264.
Japan Road Association, 2001. *Specifications for Highway Bridges, Part V, Earthquake Resistant Design*. Maruzen (in Japanese).
Kokusho, T. & Kojima, T. 2002. Mechanism for post-liquefaction water film generation in layered sand, *J. Geotechnical and Geoenvironmental Engineering* 128(2): 129–137.
Earthquake Disaster Prevention Division, National Institute for Land and Infrastructure Management. 2012. http://www.nilim.go.jp/lab/rdg/earthquake/milim-distri bution 2.zip.
Idriss, I. M. & Boulanger, R. W.2006. Semi-empirical procedures for evaluating liquefaction potential during earthquakes, *Soil Dynamics and Earthquake Engineering* 26(2–4): 115–130.
Kazama, M., Takamura, H., Unno, T., Sento, N. & Uzuoka, R. 2006. Liquefaction mechanism of unsaturated volcanic sandy soils, *J. Geotechnical Engineering, JSCE* 62(2): 546–561.
Liu, A. H., Stewart, J. P., Abrahamson, N. A. and Moriwaki, Y. 2001. Equivalent number of uniform stress cycles for soil liquefaction analysis, *J Geotechnical and Geoenvironmental Engineering* 127(12): 1017–1026.
Matsuo, O., 1999. Seismic design of river embankments. *Tsuchi-to-kiso, JGS* 47(6), 9–12 (in Japanese).
Maeda, T. & Okamura, M. 2012. Effect of thickness of saturated zone in an embankment on liquefaction induced embankment, *Prod. 47th Japan National Conference on Geotechnical Engineering, JGS* (in Japanese).
Okamura, M., Abdoun, T., Dobry, R., Sharp, M.& Taboada, V. 2001. Effects of sand permeability and weak aftershocks on earthquake-induced lateral spreading, *Soils and Foundations* 41(6): 63–78.
Okamura, M. & Inoue, T. 2010. Preparation of fully saturated model ground. *Proc. the Seventh International Conference on Physical Modelling in Geotechnics, Zurich 2010,* 1.: 147–152.
Okamura, M. & Kitayama, H. 2008. Preparation of fully saturated model ground in centrifuge and high accuracy measurement of degree of saturation. *Proc. Japanese Society of Civil Engineers* 64 (3): 662–671 (in Japanese).
Okamura, M. & Tamamura, S. 2011. Seismic stability of embankment on soft soil deposit, *Int. J. Physical Modelling in Geotechnics* 11(2): 1–8.
Okamura, M., Tamamura, S. & Yamamoto, R. 2013. Seismic stability of embankments subjected to pre-deformation due to foundation consolidation, *Soils and Foundations* 53(1), 11–22.
River Front Center, 1999. Personal Communication.
Sasaki, Y., Tamura, K., Yamamoto, M. & Ohbayashi, J. 1995. Soil improvement work for river embankment damage by 1993 Kushirooki earthquake. *Proc. the First International Conference on Earthquake Geotechnical Engineering, Tokyo* 1: 43–48.
River Bureau, Ministry of Land, Infrastructure and Transport. 2011./http://www6.river.go.jp/riverhp_viewer/entry/y2011eb4071ffc52db6d40a124e92f499b12b83125342f.htmlS.
Tanaka, T., Yasuda, S. & Naoi, K. 2009. Liquefaction and post-liquefaction deformation characteristics of some silica sands under low confining pressure, *Proc. the 30th JSCE Earthquake Engineering Symposium*.
Tohoku Regional Development Bureau, Ministry of Land, Infrastructure and Transport, 2011. /http://www.thr.mlit.go.jp/Bumon/B00097/K00360/Taiheiyouokijishinn/kenntoukai/110530/houkokusho.pdfS.
Tokimatsu, K. & Yoshimi, Y. 1983. Empirical correlation of soil liquefaction based on SPT N-value and fines content, *Soils and Foundations* 23(4): 56–74.
Tokimatsu, K. 1990. System compliance correlation from pore pressure response in undrained cyclic triaxial tests, *Soils and Foundations* 26(1): 14–22.
Tan, T.S. & Scott, R.F. 1985. Centrifuge scaling considerations for fluid particle systems. *Geotechnique* 35 (4), 461–470.
Unno, T., Kazama, M., Uzuoka, R. & Sento, N. 2008. Liquefaction of unsaturated sand considering the pore air pressure and volume compressibility of the soil particle skelton, *Soils and Foundations* 48(1): 87–100.
Yoshimi, Y., Tanaka, K. & Tokimatsu, K. 1988. Liquefaction resistance of a partially saturated sand, *Soils and Foundations* 17(1): 23–38.